RSC Advances

View Online / Journal Homepage
Dynamic Article Links

Cite this: DOI: 10.1039/c2ra20786a

www.rsc.org/advances

PAPER

Fluorescent molecular rotors under pressure: synergistic effects of an inert polymer†

Mohammed A. H. Alamiry,[a] Effat Bahaidarah,[a] Anthony Harriman,*[a] Thomas Bura[b] and Raymond Ziessel[b]

Received 26th April 2012, Accepted 22nd August 2012
DOI: 10.1039/c2ra20786a

Published on 22 August 2012 on http://pubs.rsc.org | doi:10.1039/C2RA20786A
Downloaded on 17 September 2012

Sterically unhindered boron dipyrromethene dyes bearing aryl hydrocarbons at the *meso* position can function as fluorescent probes for monitoring changes in rheology of the surrounding environment. The key aspect of such behaviour relates to the ease of rotation of the aryl ring, which is set in part by frictional forces with nearby solvent molecules. For the target dye under consideration here, gyration of the *meso*-phenylene ring shows a pronounced temperature dependence but only a modest sensitivity towards applied pressure. Changing the specific viscosity of the solvent by adding a linear polymer has but a small effect on the fluorescence yield of the dye under ambient conditions and thereby indicates that there is little contact between dye and polymer. Under pressure in the presence of polymer, the fluorescence yield increases dramatically and allows design of an effective fluorescence-based pressure sensor. The simplest explanation of this phenomenon has the polymer wrapping around the dye under pressure and curtailing the rotary action. In addition, it has to be considered that the inert polymer renders the chloroform solvent more susceptible to a pressure-induced increase in density by minimising electrostatic repulsion between chlorine lone pairs. In this respect, the polymer acts as a lubricant for compression of chloroform under pressure.

Introduction

Considerable theoretical[1–3] and experimental[4–6] attention has been directed towards understanding the role of the solvent in controlling the dynamics of barrier crossing[7] in simple molecular systems. The most widely studied processes involve light-induced conformational exchange in fluid solution at ambient pressure. Indeed, such studies have identified[8] a range of fluorescent rotors that can be applied for the *in situ* determination of local viscosity changes. Although much progress has been made in this field since the seminal contributions by Kramers in 1940,[9] our comprehension of such reactions remains rather incomplete. This is due, at least in part, to the interplay between several overlapping effects that are not easily resolved by experiment. For example, it becomes difficult to isolate polarity effects from corresponding changes in viscosity[10] and in extracting barrier heights from activation energies associated with solvent properties.[11] Even in n-alkane solvents, the isomerisation rate constant rarely exhibits the anticipated correlation with inverse viscosity.[12] This has precipitated the introduction of various models to correct for the inadequacy of bulk viscosity to depict frictional forces between solute and solvent.[13] These modifications and adaptations, while being suitable for the development of fluorescent rheology probes, fall well short of providing improved theoretical understanding. This situation also holds for the correlation of rotational diffusion times with solvent properties.

Within the generic area of rheology probes,[14] unhindered boron dipyrromethene (Bodipy) dyes have found prominent use in both biological[15] and artificial environments.[16] The key premise here is that a *meso*-phenylene ring is subjected to mild stereochemical blocking by hydrogen atoms on the dipyrrin backbone. This H,H clash hinders full rotation of the phenylene ring but does not stop the process. As a result, the fluorescence quantum yield and excited-state lifetime increase steadily with increasing viscosity of the surrounding medium, although the correlation is rarely linear.[17] It is normal practice to vary viscosity by changing the composition of the solvent or by ramping the temperature. Both effects introduce complications for data analysis. Clearly, there are benefits for covering the entire friction regime of interest using a single solvent under isothermal conditions and this can be done by applying high pressure to the system.[17] Pressure compresses[18] the solvent, raising the density and thereby affecting the viscosity. Of course, there are ancillary effects on both refractive index[19] and dielectric constant[20] that have to be taken into account. A further way to change solvent viscosity in a controlled way is to

[a]*Molecular Photonics Laboratory, School of Chemistry, Bedson Building, Newcastle University, Newcastle upon Tyne, NE1 7RU, United Kingdom. E-mail: anthony.harriman@ncl.ac.uk; Fax: 44 191222 8660; Tel: 44 191222 8660*
[b]*Laboratoire de Chimie Moléculaire et Spectroscopies Avancées (LCOSA), UMR 7515 au CNRS, Ecole Européenne de Chimie, Polymères et Matériaux, 25 rue Becquerel, 67087, Strasbourg Cedex 02, France*

† Electronic supplementary information (ESI) available: Solvent effect on photophysical properties of **ROBOD**, effect of [PMMA] on viscosity, correlation between α and the specific viscosity. See DOI: 10.1039/c2ra20786a

Published on 22 August 2012 on http://pubs.rsc.org | doi:10.1039/C2RA20786A
Downloaded on 17 September 2012

add an inert polymer.[21] The conformation of a dissolved polymer is a complex function of the properties of both solute and solvent and can be further modified by applying pressure to the system. Here, while seeking to examine how well Kramer's model[9] works with a Bodipy-based fluorescent rotor in solvent-polymer mixtures, we have encountered an unusual synergy. In particular, it is shown that adding polymer to a solution of the dye under ambient conditions has less effect on the fluorescence yield than predicted from the global change in viscosity. When subjected to applied pressure, however, the presence of the polymer causes restoration of fluorescence from the dye by switching off the rotary action. The net result is a much improved fluorescent sensor by which to monitor pressure changes at fixed temperature.

Experimental

The sterically unhindered boron dipyrromethene dye, **ROBOD**, was prepared according to Fig. 1 and details are provided below. In short, the synthesis proceeds in two steps starting from the condensation of freshly distilled pyrrole (in excess) with 4-bromobenzaldehyde in the absence of oxygen.[22] This reaction leads to the dipyrromethane dye **1** which could be purified easily by flash column chromatography on silica. The second step consists in oxidation of the dipyrromethane to the corresponding dipyrromethene using DDQ as oxidant, followed by the *in situ* complexation of boron(III). The nascent acid is quenched by triethylamine.[23] The target dye was obtained in 43%, after chromatography and subsequent recrystallization. The **BODIPY** dye used as a control compound was prepared and purified according to a literature procedure.[24] NMR spectroscopy, MS and elemental analysis unambiguously confirm the molecular structures of these synthetic dyes. It might be noted that the bromine atom present in **BODIPY** plays no part in determining the photophysical properties; its primary function is to provide an anchor by which to attach the dye to macromolecular supports.

Preparation and characterisation of the dipyrrin 1

Freshly distilled pyrrole (30 mL, 25 equiv.) and 4-bromobenzaldehyde (2.80 g, 1.0 equiv.) were added to a dry, round-bottomed flask and degassed with a stream of Ar for 5 min. Trifluoroacetic acid (126 μL, 0.10 equiv.) was then added, and the solution was stirred under Ar at room temperature for 5 min before being quenched with 0.1 M NaOH. Ethyl acetate was then added. The organic phase was washed with water and dried over anhydrous Na_2SO_4, and the solvent was removed under vacuum to afford an orange-brown oil. Excess of pyrrole was removed by vacuum distillation. Afterwards, the crude material was purified by flash column chromatography (SiO_2 petroleum ether/ethyl acetate 90/10) to afford compound **1** (3.10 g, 60%). ^{1}H NMR ($CDCl_3$, 200 MHz): 5.44 (s, 1H), 5.89 (s, 2H), 6.15–6.19 (m, 2H), 6.70–6.73 (m, 2H), 7.09 (d, 2H, ^3J = 8.3 Hz), 7.43 (d, 2H, ^3J = 8.8 Hz), 7.92 (br, s, 1H).

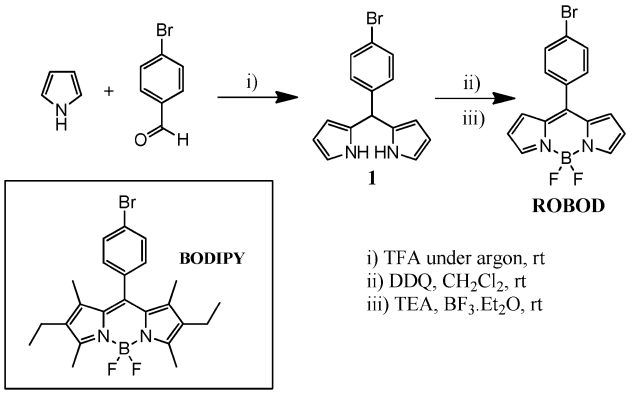

Fig. 1 Synthetic scheme used for the preparation of the unsubstituted dye, **ROBOD**. The inset gives the chemical formula of the substituted dye, **BODIPY**.

Preparation and characterisation of the ROBOD

A round-bottomed flask was charged with compound **1** (3.1 g, 10.3 mmol) in freshly distilled CH_2Cl_2 (150 mL), and the solution was purged with argon in the dark for 45 min. Dichlorodicyanobenzoquinone (7.000 g, 31 mmol) was added and the solution stirred at room temperature in the dark for 1.5 h. After confirmation by thin layer chromatography (silica gel plate, CH_2Cl_2) that all the dipyrromethane had been consumed, triethylamine (8.6 mL, 62 mmol) and boron trifluoride-diethyl ether (10.5 mL, 82.4 mmol) were added dropwise under argon. The resultant dark brown solution was stirred in the dark for 20 h, until full consumption of the intermediate was confirmed by thin layer chromatography. The reaction mixture was subsequently diluted with CH_2Cl_2 and washed with brine. The separated organic layer was dried with anhydrous magnesium sulfate. The organic layers were concentrated under reduced pressure, and the resultant red/black solid was purified by flash column chromatography (silica gel; petroleum ether/ethyl acetate, 9 : 1) to afford **ROBOD** (1.53 g 43%). ^{1}H NMR ($CDCl_3$, 300 MHz): 6.57 (d, 2H, ^3J = 4.2 Hz), 6.92 (d, 2H, ^3J = 4.2 Hz), 7.45 (d, 2H, ^3J = 8.1 Hz), 7.69 (d, 2H, ^3J = 8.4 Hz), 7.96 (s, 2H). ^{13}C NMR ($CDCl_3$, 50 MHz): 145.8, 144.6, 134.7, 132.6, 131.8, 131.3, 125.5, 118.9. EI-MS 346.0 ([M], 100). Elemental analysis for $C_{15}H_{10}BBrF_2N_2$: calc, C, 51.92, H, 2.91, N, 8.07; found; C, 51.75, H, 2.68, N, 7.84.

Absorption spectra were recorded with a Hitachi U3310 spectrophotometer and fluorescence spectra were recorded with a Hitachi F-4500 emission spectrophotometer. All fluorescence spectra were fully corrected for spectral imperfections of the instrument on the basis of a standard lamp. Emission quantum yields and excited-state lifetimes were measured[17a] as reported previously for closely related dyes. All optical studies were made with dilute solutions after filtration to ensure removal of any particulate material. Low temperature studies were made with the sample sealed under N_2 into an optical cell and housed within the chamber of an Oxford Instruments Optistat-4. Various excitation wavelengths were used for each sample and all emission spectra were supported by comparing fluorescence and excitation spectra recorded with comparable slit widths. Experiments were repeated several times.

The high-pressure rig was purchased from Stansted Fluid Power Ltd. The general layout comprises a hydraulic compressor constructed from stainless steel. Ethanol is used as the hydraulic medium. The two-stage pump is fitted with an intensifier and

This journal is © The Royal Society of Chemistry 2012

Published on 22 August 2012 on http://pubs.rsc.org | doi:10.1039/C2RA20786A
Downloaded on 17 September 2012

diaphragm compressor capable of reaching about 700 MPa. The sample chamber has been machined from a block of stainless steel and is equipped with three optical windows and a Bourdon pressure gauge. The windows show good transmission at wavelengths longer than 370 nm. For absorption measurements, the sample chamber is connected to a Perkin-Elmer lambda-5 spectrophotometer using input and output optical fibre bundles. The absorbance signal is calibrated by reference to the sample solution being recorded in conventional cuvettes with background subtraction. For emission studies, an appropriate laser diode is used as excitation source and output collected at 90° to excitation is directed to the spectrofluorimeter with an optical fibre bundle. Purpose-made cells are used to accommodate liquid samples of appropriate concentration. For fluorescence studies, the sample cell is a glass tube, diameter *ca.* 4 mm, having a narrow mouth that can be capped with a poly(ethylene) seal. The latter takes the form of a short tube that is heat-sealed at one end. For absorption measurements, a hollow glass disk fitted with a narrow inlet tube is used to hold the sample. This disk has a diameter of *ca.* 1 cm and a pathlength of 2 mm. Again, a poly(ethylene) tube is used as stopper for the cell and the actual pathlength can be calibrated by absorption spectroscopy. Sample cells and poly(ethylene) seals are used once and then discarded.

In a typical experiment, a solution of the relevant compound was prepared (usually in methyltetrahydrofuran (MTHF) but sometimes in $CHCl_3$) and the concentration adjusted appropriately; absorption spectral measurements were made with an absorbance of *ca.* 0.50 at the peak maximum and fluorescence studies were carried out with an absorbance of *ca.* 0.05 at the excitation wavelength. Spectra were recorded at atmospheric pressure and compared with those obtained under conventional conditions using optical cuvettes. The pressure was increased in small jumps, the sample equilibrated at each pressure, and the spectrum recorded. Having reached the maximum pressure, this being restricted to 550 MPa for safety reasons, the pressure was released and spectra recorded to ensure full reversibility of any effects. In other experiments, the pressure was raised to 550 MPa and released slowly with spectra being recorded at each stage. To check for self-consistency, spectra were recorded at certain pressures after leaving the sample for prolonged periods at that pressure. All measurements were repeated using fresh solutions and, for emission studies, different excitation wavelengths. Data analysis included making background corrections, especially for absorption measurements, and averaging several spectra recorded under the same conditions.

Results and discussion

Photophysical properties

The starting point for this investigation lies with the unhindered Bodipy dye, **ROBOD**, which is a member of a well-known class of viscosity probes.[17a] In MTHF at room temperature, **ROBOD** displays a strong absorption transition with a clear maximum at 502 nm, and a much weaker set of absorption transitions stretching across the near-UV region. Fluorescence is observed, with a maximum at 530 nm in MTHF, and shows reasonable mirror symmetry with the lowest-energy absorption band (Fig. 2). The Stokes' shift of 1050 cm^{-1} is modest and attests to minor structural distortion accompanying population of the

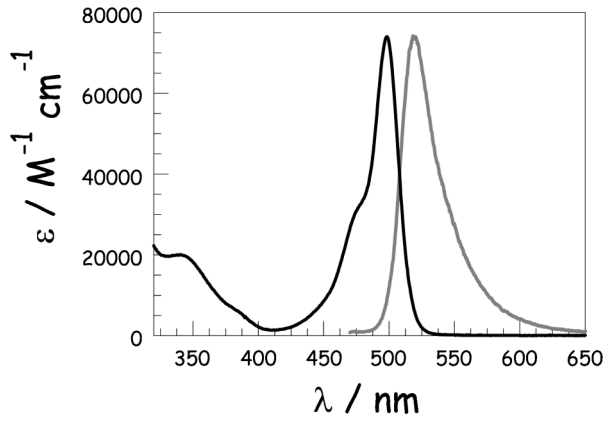

Fig. 2 Absorption spectrum (black line), presented in terms of the molar absorption coefficient (ε), and the normalised fluorescence spectrum (grey curve) recorded for **ROBOD** in MTHF at room temperature.

first-excited singlet state.[25] The phenylene ring gyrates around the connecting single bond,[16a] causing slight buckling of the dipyrrin backbone, in fluid solution at ambient temperature. In turn, this rotary effect enhances nonradiative decay of the first-excited-singlet state and causes a pronounced loss of fluorescence. The significance of the rotary action can be gauged by comparing the photophysical properties of **ROBOD** with those of the sterically blocked analogue, **BODIPY**, where the only important structural change relates to the presence of methyl groups at the 3,5-positions.

It might be argued that these methyl groups are not sufficiently bulky to prevent rotation of the phenylene ring. Certainly, the ring will gyrate about a mean position and molecular dynamics simulations made *in vacuo* can be used to suggest that infrequent full rotation takes place. Related dyes studied by Lindsey and coworkers[16a] having blocking methyl groups on the 2,6-positions of the phenylene ring but no dipyrrin substituents do behave as molecular rotors, albeit ineffective ones. Also, Kuimova *et al.*[15c] have reported a clear dependence of the fluorescence quantum yield on the availability of methyl groups at the *meso*-phenylene and/or dipyrrin unit. Furthermore, we show below that the nonradiative rate constant determined for **BODIPY** contains an activated component that could reflect rotation of the *meso*-phenylene ring. To ensure that **BODIPY** fulfills its role as a control compound, we have recorded the pressure-induced absorption and fluorescence spectral changes for perylene,[20] where internal rotation cannot take place. Such critical comparison indicates that **BODIPY** is, at best, a very poor molecular rotor under our conditions.

Table 1 lists the absorption (λ_{MAX}) and emission (λ_{FLU}) maxima recorded for the two dyes in MTHF at room temperature. The slight shifts are due to the inductive effect of the alkyl substituents. Also shown are fluorescence quantum yields (Φ_F), singlet-excited state lifetimes (τ_S), radiative (k_{RAD}) and nonradiative (k_{NR}) rate constants and Stokes' shifts (Δ_{SS}) for the two compounds recorded under identical conditions. It can be seen that whereas nonradiative decay is relatively unimportant for **BODIPY**, it is the dominant deactivation route for **ROBOD**. Comparable results are found in a small range of other solvents (see ESI†) and there are no obvious effects of

Published on 22 August 2012 on http://pubs.rsc.org | doi:10.1039/C2RA20786A
Downloaded on 17 September 2012

Table 1 Summary of photophysical properties recorded for the two fluorophores of interest in MTHF solution.

Property	ROBOD	BODIPY
λ_{MAX}/nm [a]	502	525
λ_{FLU}/nm [a]	530	547
Φ_F [a]	0.023	0.72
τ_S/ns [a]	0.15	4.8
Δ_{SS}/cm^{-1}	1050	765
k_{RAD}/10^8 s^{-1} [a]	1.5	1.5
k_{NR}/10^7 s^{-1}	630	0.06
k_{NR}^0/10^7 s^{-1}	6.2	2.8
k_{ACT}/10^{11} s^{-1}	5.2	110
E_A/kJ mol^{-1}	11.0	31.1

[a] Refers to room temperature.

solvent polarity on the photophysical properties of these compounds.[26]

To confirm that the enhanced nonradiative decay of **ROBOD** is due to the rotor effect, the emission properties of both compounds were recorded in MTHF as a function of temperature. In accordance with the Englman–Jortner energy-gap law,[27] fluorescence from **BODIPY** is quite insensitive to changes in temperature over the range from 77 to 300 K. However, Φ_F recorded for **ROBOD** increases markedly as the temperature decreases and becomes comparable to that of **BODIPY** below the freezing point of the solvent (Fig. 3). As the temperature falls, the emission profile narrows slightly but does not undergo a significant spectral shift until the solvent freezes at *ca.* 150 K. On forming a glassy matrix at *ca.* 100 K, the fluorescence profile sharpens further and undergoes a small blue shift. Comparable spectral changes are found for **BODIPY** but here Φ_F increases only slightly (*i.e.*, <10%) as the temperature decreases.

$$k_{NR} = k_{NR}^0 + k_{ACT} e^{-\frac{E_A}{RT}} \quad (1)$$

For both dyes, the nonradiative rate constant falls smoothly as the temperature drops and can be explained quantitatively in terms of eqn (1) where k_{NR}^0 is a temperature independent rate constant that tends to dominate in the glassy region, k_{ACT} is an activated rate constant for nonradiative decay in the liquid phase, and E_A is the activation energy for the latter process (Fig. 4). The derived parameters for the two dyes are collected in Table 1. It might be considered that the activationless rate constant included in eqn (1) is redundant, especially in the liquid phase, although it must improve the overall quality of the fit. When extending the fit to include the frozen and glassy states (MTHF freezes at about 147 K but does not form an optical glass until around 100 K) the fit demands inclusion of k_{NR}^0. This latter term includes intersystem crossing to the triplet manifold and vibrational relaxation to the ground state. Both of these processes should be activationless.[27] It is not possible to simply ascribe the activated step to rotation of the phenylene ring (*i.e.*, the rotary action that underpins the ability of **ROBOD** to monitor local viscosity) because the exact nature[16a] of the excited-singlet state potential energy curve is not known. It is likely that, in these unconstrained Bodipy derivatives, more than one structural motion is linked to nonradiative decay. Even for **BODIPY**, the fit to the experimental data collected over the full temperature range requires both k_{ACT} and k_{NR}^0.

It can be seen that whereas k_{NR}^0 is similar for the two compounds, there are significant differences in the activated terms. Thus, the temperature-dependence studies indicate that **ROBOD** is characterised by a relatively small activation barrier of *ca.* 11 kJ mol^{-1}. This barrier is believed to correspond to gyration of the phenylene ring around the dipyrrin backbone and is unavailable for the sterically-locked dye; as such, E_A includes an important contribution from the temperature effect on the viscosity of the solvent. For **BODIPY**, a much higher barrier of *ca.* 31 kJ mol^{-1} is found and this is difficult to cross at ambient temperature. The origin of this barrier is far from obvious but might also involve some type of ring rotation in the excited state. Note that intersystem crossing to the triplet manifold is relatively unimportant for both dyes. This point becomes significant when designing practical systems since triplet formation promotes generation[28] of singlet molecular oxygen.

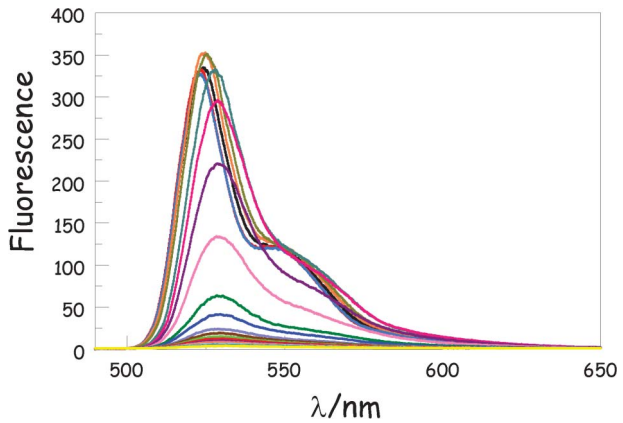

Fig. 3 Effect of temperature on the fluorescence spectrum of **ROBOD** in MTHF; temperatures range from 290 K to 80 K in increments of 10 K. The emission intensity increases as the temperature falls while there is a sharpening and small blue shift once the solvent starts to freeze. See text for a full description of these effects.

Effect of increased viscosity

In principle, the barrier to internal rotation of the *meso*-phenylene ring present in **ROBOD** should increase with

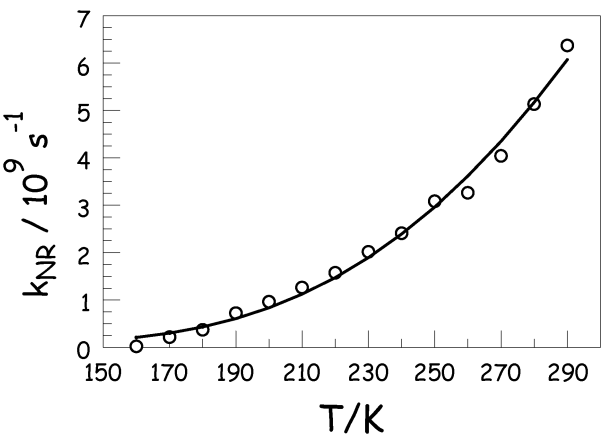

Fig. 4 Effect of temperature on the rate constant for nonradiative decay of **ROBOD** in MTHF. The parameters derived from the fit to eqn (1) (solid line) to the experimental data (circles) are given in Table 1.

This journal is © The Royal Society of Chemistry 2012

Published on 22 August 2012 on http://pubs.rsc.org | doi:10.1039/C2RA20786A
Downloaded on 17 September 2012

increasing viscosity of the surrounding solvent, although the effect might be non-linear[17] and more correctly described in terms of microviscosity. Two experiments were made in order to assess this situation with **ROBOD** in chloroform; the change in solvent being necessitated by the need to add an inert polymer, namely poly(methylmethacrylate), PMMA. Firstly, the effects of added PMMA (molar mass = 140 000 g mol^{-1}, density = 1.185 g cm^{-3}) on the fluorescence yield of **ROBOD** were explored under ambient conditions. In fact, Φ_F is hardly affected by the presence of high concentrations of polymer as can be seen from Fig. 5. There is a small increase in Φ_F with increasing PMMA content, amounting to a change from 0.036 to 0.043 on addition of a high concentration (*i.e.*, 25% w/v) of PMMA. This corresponds to a decrease in k_{NR} of *ca.* 20%. Within experimental limitations, this increase is linear with respect to PMMA concentration, although there is considerable spread of the data caused by the relative insensitivity. The presence of PMMA raises the viscosity of the solution by a significant amount[29] (see ESI†). Although it is known[17] that **ROBOD** responds to changes in local viscosity, as adjusted by changing the nature of the bulk solvent, this appears not to be the case when the viscosity is altered[30] by addition of a linear polymer; the shear viscosity increases from 0.563 mPa s in the absence of polymer to 3.21 mPa s for the highest concentration of PMMA used here. When the same change in viscosity is realised by changing the nature of the solvent, Φ_F increases by 2.15-fold at 20 °C.

The inference to be drawn from this observation is that **ROBOD** remains in the $CHCl_3$ solvent and does not interact significantly with the polymer. As such, its fluorescence behaviour is somewhat isolated from the full rheological effects of the added PMMA. Likewise, the presence of polymer has no effect on either absorption or fluorescence maximum in $CHCl_3$ solution. Comparable behaviour was found for **BODIPY** under the same conditions where the presence of PMMA has essentially no effect on the fluorescence quantum yield or optical properties.

In the second experiment, we examined the effect of applied pressure on the fluorescence properties of **ROBOD** in $CHCl_3$ at 20 °C. Under such conditions, the density (ρ = 1.483 g cm^{-3}) of $CHCl_3$ increases and its freezing point, which occurs at −63.5 °C at atmospheric pressure, is elevated to room temperature under an applied pressure of 0.6 to 0.8 GPa.[31] The magnitude of the pressure-induced density change can be monitored by following the absorbance at the maximum of the S_0-S_1 absorption transition (Fig. 6). There is a progressive increase in absorbance with applied pressure that amounts to a factor of *ca.* 20% over a pressure range of 0–550 MPa. Because of this latter effect, there is also a small change in polarisability of the solvent[32] which, in turn, causes a substantial red shift for both absorption and fluorescence maxima recorded for **ROBOD**; these shifts amount to *ca.* 15 nm for a pressure increase to 550 MPa. Over the same pressure range, there is a substantial increase in Φ_F which, after correction for compression of the solvent, amounts to an increase from 0.034 at atmospheric pressure to 0.092 at 550 MPa (Fig. 7). Before attempting analysis of these data it is prudent to consider similar experiments made for the control dye.

Thus, applied pressure causes an increase in absorbance and small red shift for the peak maximum for **BODIPY** in MTHF at room temperature; *N.B.* the effects of pressure on the properties of MTHF have been described earlier.[20] There is a similar red shift for the fluorescence maximum and a small increase in Φ_F, after correction for the density change. This modification of Φ_F is due to a pressure-induced increase in the solvent refractive index and therefore a corresponding increase in k_{RAD} (Fig. 8a). This conclusion is supported by the observation that the nonradiative rate constant, k_{NR}, is insensitive to changes in applied pressure over the full range (Fig. 8b). Unlike **ROBOD**, the constrained Bodipy dye is, at best, a poor molecular rotor under these conditions. To be sure on this point, a further series of control experiments were made with perylene (Φ_F = 0.88 and τ_S = 5.9 ns at atmospheric pressure) in MTHF, where there is no possibility for internal rotation. The derived data are shown on Fig. 8. Increased pressure causes a very slight increase in Φ_F (Fig. 8a) due to the effect on k_{RAD} but no change in k_{NR} (Fig. 8b).

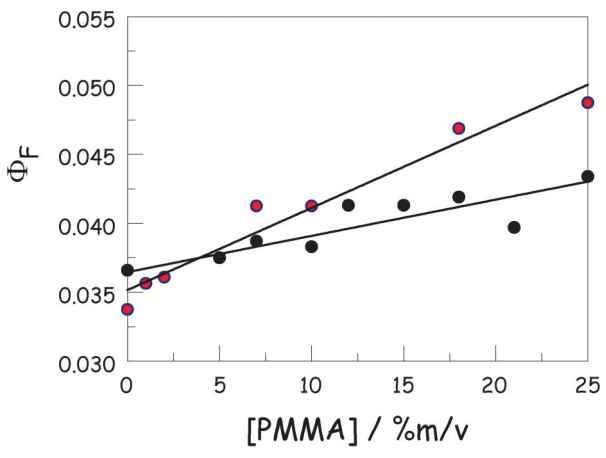

Fig. 5 Effect of added PMMA on the fluorescence quantum yield of **ROBOD** in $CHCl_3$ at 20 °C. Experimental points correspond to a titration with PMMA (black circles) and interpolation of the pressure-sensitive studies (red circles). In both cases, the solid line is a least-squares fit to a linear expression.

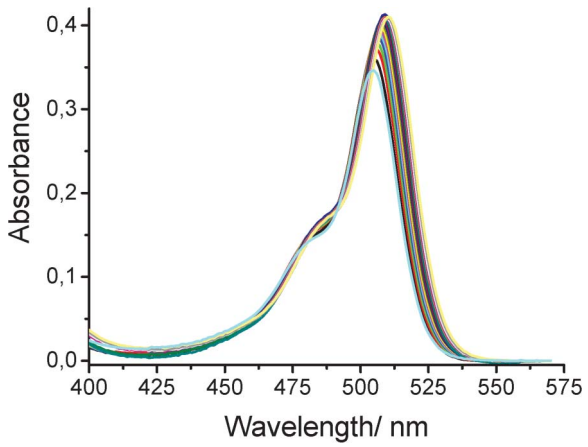

Fig. 6 Effect of applied pressure on the absorption spectral profile recorded for **ROBOD** in $CHCl_3$ at room temperature. The pressure is varied from atmospheric pressure to 550 MPa in increments of 27.5 MPa. The absorbance increases progressively with increasing pressure while the peak maximum undergoes a small red shift due to the change in polarizability.

Published on 22 August 2012 on http://pubs.rsc.org | doi:10.1039/C2RA20786A
Downloaded on 17 September 2012

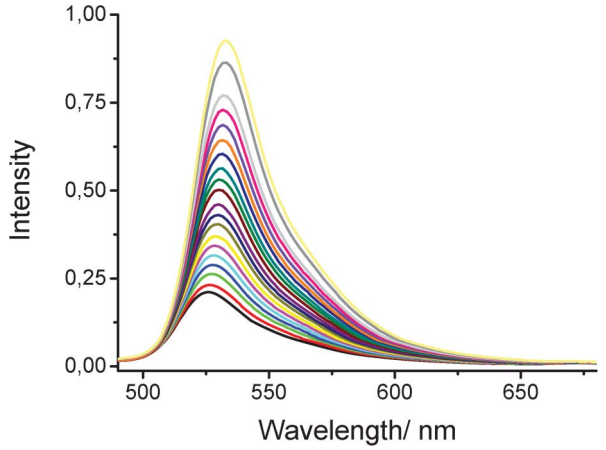

Fig. 7 Effect of applied pressure on the fluorescence spectral profile recorded for **ROBOD** in $CHCl_3$ at room temperature. The pressure is varied from atmospheric pressure to 550 MPa in increments of 27.5 MPa. The emission intensifies progressively with increasing pressure while the peak maximum undergoes a small red shift due to the change in polarizability. The excitation wavelength was 406 nm.

Now we return to the pressure effect on Φ_F observed for **ROBOD** in $CHCl_3$ (Fig. 8a). The entire curve can be fit to a power law expression of the type shown by eqn (2) where A and B are constants and C is the power coefficient. This expression implies that there is a limiting Φ_F ($A = 0.033$) at low pressure and a pressure moderator ($B = 110$ MPa^{-1}). The derived value for the coefficient ($C = 1.0$) indicates that Φ_F evolves linearly with applied pressure, which is somewhat surprising in that pressure

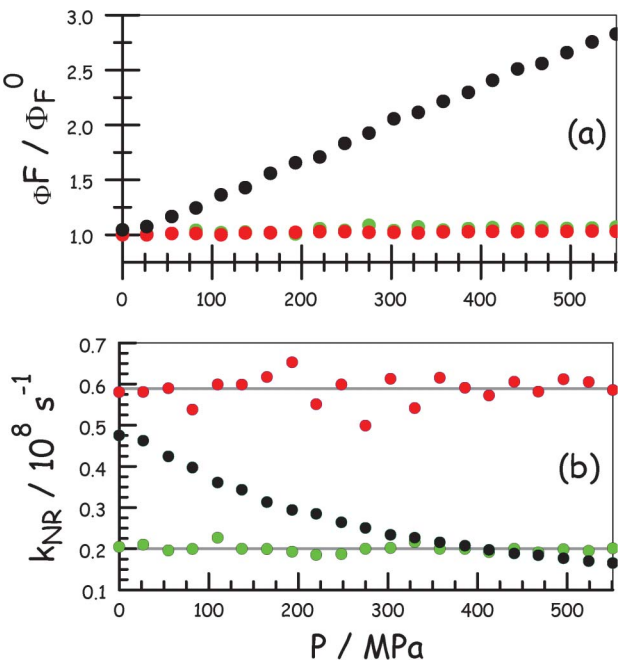

Fig. 8 Effect of applied pressure on the derived photophysical properties for **ROBOD** (black), **BODIPY** (red) and perylene (green) in MTHF at room temperature. (a) Relative fluorescence quantum yield where Φ_F^0 refers to atmospheric pressure. (b) Nonradiative decay rate constant where the values for ROBOD are divided by 100 for convenient comparison.

exerts an effect on both k_{RAD}, because of the refractive index modulation, and k_{NR}. Perhaps, the apparent linearity reflects the fact that k_{NR} dominates the deactivation process for this system. It is also to be expected that Φ_F will become independent of pressure at very high pressure, or more correctly as Φ_F approaches unity, but we are unable to access this range.

$$\Phi_F = A + (BP)^C \quad (2)$$

For **ROBOD** in $CHCl_3$ at room temperature, pressure affects k_{NR} in a nonlinear manner (Fig. 8b). This is not so surprising because pressure has several simultaneous effects on factors affecting the fluorescence yield; *e.g.*, increasing frictional forces, bending the dipyrrin backbone and modifying the shapes of ground- and excited-state potential energy surfaces. We attribute the general effect to inhibition of the rotary action[33] caused by closer packing of solvent molecules under pressure. At relatively high pressure ($P > 200$ MPa), a log–log plot for k_{NR} *vs.* P is linear with a gradient of -0.60. This is interesting in as much as Kramers' theory[9] predicts a corresponding linear log–log plot for k_{NR} *vs.* viscosity, where the usual gradient is roughly -0.67. We do not know the precise relationship between pressure and viscosity for $CHCl_3$ but such correlations are often linear and, as such, the high-pressure behaviour illustrated for **ROBOD** on Fig. 8b seems reasonable. In the low pressure region, k_{NR} tends towards a pressure-independent value that must correspond to a regime where viscosity no longer controls the dynamics of ring rotation. Again, this situation is fully consistent with Kramers' theory.[9]

Effects of applied pressure in the presence of added PMMA

It will be recalled that addition of PMMA has little effect on the absorption or emission properties of these dyes in $CHCl_3$ solution. There seems to be no real attraction between dye and polymer in this solvent under ambient conditions. Indeed, control experiments made with **BODIPY** and perylene in $CHCl_3$ containing PMMA (5% mass per volume) gave results strikingly similar to those obtained in the absence of polymer. The main difference is that solutions containing high concentrations of PMMA are more compressible than is pure $CHCl_3$ at ambient temperature. This has important consequences for the local viscosity which, at any given pressure, is elevated by the presence of polymer. It could be that PMMA acts as a screen to overcome repulsive interactions between lone pairs on the chlorine atoms as the solvent compresses. Taking due account of the density change under applied pressure, we conclude that PMMA has little effect on the photophysical properties of these two control dyes. However, on raising the pressure in the presence of PMMA fluorescence from **ROBOD** becomes more noticeable and, in particular, Φ_F increases steadily with increasing pressure (Fig. 9 and ESI†).

The rate of increase of Φ_F with applied pressure is significantly more pronounced in the presence of PMMA. The net effect of pressure on Φ_F can be described in terms of eqn (2),[34] although the apparent linearity seen in the absence of polymer is lost. Indeed, at high concentrations (>5% mass per volume) of PMMA the derived profiles are clearly curved. It is recognised that the specific viscosity[35] of the solution increases linearly with increasing mass percent of PMMA in $CHCl_3$ and throughout the

This journal is © The Royal Society of Chemistry 2012

Published on 22 August 2012 on http://pubs.rsc.org | doi:10.1039/C2RA20786A
Downloaded on 17 September 2012

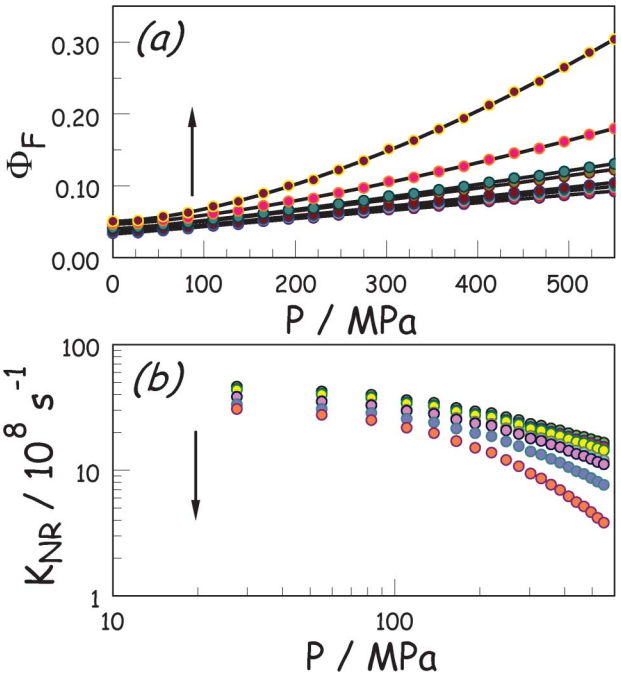

Fig. 9 Effect of applied pressure for **ROBOD** in MTHF containing PMMA at 20 °C: [PMMA] values are 0, 1, 2, 5, 10, 18 and 25% m/v. (a) The effect of applied pressure on the fluorescence quantum yield where the solid line is a fit to eqn (2). (b) The effect of pressure on the nonradiative decay rate constant. In each case, the arrow indicates the direction of increasing [PMMA].

range of PMMA concentrations, the value determined from the fit for the parameter A agrees well with that expected for the emission quantum yield in the presence of PMMA at atmospheric pressure (Table 2). These data are shown on Fig. 5 and lead to an improved understanding of how polymer concentration affects the fluorescence yield. As observed for the direct titration experiment, Φ_F appears to evolve in a linear manner with added polymer, although the overall effect is modest and the high level of experimental uncertainty precludes close scrutiny of the fit. The two sets of data are reasonably consistent, although the fits diverge at high concentration of PMMA, and confirm that the presence of polymer does not, by itself, have much effect on the fluorescence quantum yield of the dye in $CHCl_3$ solution.

Table 2 Parameters associated with the effects of applied pressure on the photophysical properties of **ROBOD** at 20 °C in $CHCl_3$ containing PMMA.

[PMMA]^a	A^b	B/MPa^{-1}	C	α^c
0	0.033	110	1.01	−0.59
1	0.034	130	1.04	−0.62
2	0.035	160	1.10	−0.66
5	0.040	225	1.20	−0.73
10	0.040	250	1.20	−0.77
18	0.046	430	1.40	NA
25	0.050	760	1.58	NA

^{a} Concentration of added PMMA expressed in terms of % mass to volume. ^{b} Corresponds to the limiting Φ_F in the absence of PMMA and at atmospheric pressure. ^{c} Corresponds to the gradient of a log–log plot of pressure *vs.* k_{NR}.

The remaining terms in eqn (2),[34] namely the pressure moderator B, having units of inverse pressure, and the power coefficient C, increase systematically with increasing concentration of PMMA (Table 2). These two terms are likely correlated by the analysis but separating B from the power coefficient (*i.e.*, $\Phi_F = A + BP^C$) does not change the situation. Attempting to restrict either B or C to the value derived without added PMMA fails to fit the experimental data; quite clearly C must increase throughout the data set to account for the observed curvature, but poor fits arise when fixing B. One feature to bear in mind is that pressure affects both k_{RAD} and k_{NR}, as mentioned earlier, but is acerbated as Φ_F increases. It is also important to stress that Φ_F must start to level out to a maximum value at very high pressure. This behaviour, which is not seen is our experiments, is not predicted by eqn (2).

It might be recalled that, within experimental limits, Φ_F increases linearly with specific viscosity and it is known[36] that the rotational relaxation time (τ_R) of $CHCl_3$, measured by NMR or FTIR spectroscopy at 303 K, increases progressively over the pressure range of interest to our studies. In turn, τ_R is expected to evolve in a first-order manner with shear viscosity divided by absolute temperature.[37] We can use this information to suggest that the observed pressure effect is not a simple consequence of increased shear viscosity. Rather, the evolution of Φ_F seen here (Fig. 9) is unique to the application of pressure in the presence of PMMA.

The effect of applied pressure on k_{RAD} in the presence of PMMA is unknown and therefore it is not possible to make the same kind of analysis for k_{NR} as outlined above in the absence of polymer. At low concentrations of PMMA, log–log plots do show a linear region at high pressure when k_{RAD} is taken to be that measured in pure $CHCl_3$ but the gradient (α) decreases slightly with increasing amount of polymer (Table 2). This linearity disappears at high polymer concentrations.

Now, the overall effect is quite pronounced in as much as the combination of applied pressure and added PMMA restores fluorescence from **ROBOD** but not to the level found for **BODIPY**. At 550 MPa in the presence of 25% m/v PMMA, Φ_F reaches 0.30 which represents an increase of almost 9-fold relative to pure $CHCl_3$ at atmospheric pressure. Under the same conditions, Φ_F for **BODIPY** increases by <5%. Thus, PMMA and pressure act in synergy to enhance fluorescence from **ROBOD** and it is natural to attribute this situation to blocking of the rotary motion of the phenylene ring. The simplest explanation for this effect can be summarised as follows: under pressure, the polymer starts to coil as a means by which to relieve the stress, most notably satisfying the need to lower the volume of the solution, and this structural change will entrap dye within the network. Close contact between polymer and dye will severely hinder rotation of the phenylene ring, cutting off nonradiative decay and restoring fluorescence. The net effect would be to coat the dye with a surrounding layer of plastic. Although attractive, this argument does not take due account of the known pressure effect on certain polymer solutions.[38]

It should be recognised that $CHCl_3$ is a good solvent for PMMA and, as such, the polymer will persist in a relatively extended conformation.[39] The fluorescent dye remains in the $CHCl_3$ such that its spectroscopic properties are insensitive to the presence of PMMA. Compression of the solution will lead to

Published on 22 August 2012 on http://pubs.rsc.org | doi:10.1039/C2RA20786A
Downloaded on 17 September 2012

a marked escalation in PMMA concentration as the density increases but there is little evidence in the scientific literature to indicate that the radius of gyration of an added polymer changes with pressure.[40] The increased friction that accompanies the application of high pressure, therefore, is considered to arise from two complementary effects. Firstly, as the density of the solvent increases there is a concomitant increase in the concentration of the polymer and, in turn, this raises the viscosity. This situation is aided by the polymer chains serving to isolate $CHCl_3$ molecules such that there is less resistance towards compression and, at a given pressure, the density is higher in the presence of PMMA. Secondly, pressure modifies the extent of interaction between dye and polymer. In the limiting case, this could lead to the polymer coating the dye. Since pressure affects each individual part of the system (*i.e.*, dye, solvent and polymer) to differing degrees, it is not unreasonable that the power coefficient C exceeds unity or that the moderator term B depends on the composition of the mixture.

Conclusions

It might be possible to develop the molecular system described here as a simple but effective pressure sensor at ambient temperature. Such materials could be applicable for the routine detection of pressure, or accompanying viscosity, under hazardous or remote conditions. For example, lubrication usually involves the subjection of a polymer solution to very high pressures for extended periods under circumstances where it is difficult to make real-time measurements. Exposure to high pressures has no long-term effect on the fluorescence properties of the dyes used herein and control studies can be made with dyes unable to undergo internal rotation. The change in rheological properties of macromolecular solutions under applied pressure is a subject of considerable industrial importance but it presents severe challenges to both theory and rigorous experimental study. We consider this investigation as being a starting point for a detailed examination of the subject.

A complicating issue in terms of sensor development is that the nonradiative rate constant depends on temperature. The actual relationship is complex and, at least for the present case, cannot be attributed to specific effects. There are at least three factors involved; viscosity, internal rotation, and backbone twisting. In this work, the activation studies are given only to indicate the rotor effect and the temperature dependence is treated globally. It is also important to stress that a more complete understanding of how pressure affects the rotary action of the sensor is needed. Indeed, eqn (2) needs to be replaced with a version that accounts for very high pressures and for which the parameters B and C can be assigned to physical terms. This is particularly so for the interaction between polymer and rotor. At present this is not the case but, to the best of our knowledge, this is the first report of a combined (solvent and polymer) system and there are many variables that need to be examined before firm mechanistic conclusions can be drawn.

Acknowledgements

We thank Newcastle University, the Université Louis Pasteur de Strasbourg, the CNRS and EPSRC for financial support of this work. EB thanks King Abdulaziz University of Saudi Arabia for financial support.

References

1 S. P. Velsko, D. H. Waldeck and G. R. Fleming, *J. Chem. Phys.*, 1983, **78**, 249–258.
2 M. Olivucci, I. N. Ragazos, F. Bernardi and M. A. Robb, *J. Am. Chem. Soc.*, 1993, **115**, 3710–3721.
3 W. P. Keirstead, K. R. Wilson and J. T. Hynes, *J. Chem. Phys.*, 1991, **95**, 5256–5267.
4 S. P. Velsko and G. R. Fleming, *J. Chem. Phys.*, 1982, **76**, 3553–3562.
5 K. C. Hasson, F. Gai and P. A. Anfinrud, *Proc. Natl. Acad. Sci. U. S. A.*, 1996, **93**, 15124–15129.
6 T. Asano, H. Furuta and H. Sumi, *J. Am. Chem. Soc.*, 1994, **116**, 5545–5550.
7 S. K. Kim, S. H. Courtney and G. R. Fleming, *Chem. Phys. Lett.*, 1989, **159**, 543–548.
8 (*a*) M. A. Haidekker and E. A. Theodorakis, *Org. Biomol. Chem.*, 2007, **5**, 1669–1678; (*b*) M. K. Kuimova, G. Yahioglu, J. A. Levitt and K. Suhling, *J. Am. Chem. Soc.*, 2008, **130**, 6672–6673.
9 J. E. I. Korppi-Tommola, A. Hakkarainen, T. Hukka and J. Subbi, *J. Phys. Chem.*, 1991, **95**, 8482–8491.
10 (*a*) J. K. Rice and A. P. Baronavski, *J. Phys. Chem.*, 1992, **96**, 3359–3366; (*b*) F. Zhou, J. Shao, Y. Yang, J. Zhao, H. Guo, X. Li, S. Ji and Z. Zhang, *Eur. J. Org. Chem.*, 2011, 4773–4787; (*c*) J. Shao, S. Ji, X. Li, J. Zhao, F. Zhou and G. Guo, *Eur. J. Org. Chem.*, 2011, 6100–6109.
11 T. Scherer, I. H. M. Van Stokkum, A. M. Brouwer and J. W. Verhoeven, *J. Phys. Chem.*, 1994, **98**, 10539–10549.
12 S. P. Velsko and G. R. Fleming, *Chem. Phys.*, 1982, **65**, 59–70.
13 L. A. Chen, R. E. Dale, S. Roth and L. Brand, *J. Biol. Chem.*, 1977, **252**, 2163–2169.
14 (*a*) J. Szymanski, A. Patkowski, A. Wilk, P. Garstecki and R. Holyst, *J. Phys. Chem. B*, 2006, **110**, 25593–25597; (*b*) Y. Wang, A. Warshawsky, C. Y. Wang, N. Kahana, C. Chevallard and V. Steinberg, *Macromol. Chem. Phys.*, 2002, **203**, 1833–1843; (*c*) S. Muller, M. Donner and J. F. Stoltz, *Biorheology*, 1986, **23**, 285–290.
15 (*a*) J. A. Levitt, M. K. Kuimova, G. Yahioglu, P. H. Chung, K. Suhling and D. Phillips, *J. Phys. Chem. C*, 2009, **113**, 11634–11642; (*b*) J. A. Levitt, P. H. Chung, M. K. Kuimova, G. Yahioglu, Y. Wang, J. L. Qu and K. Suhling, *ChemPhysChem*, 2011, **12**, 662–672; (*c*) M. K. Kuimova, G. Yahioglu, J. A. Levitt and K. Suhling, *J. Am. Chem. Soc.*, 2008, **130**, 6672–6673.
16 (*a*) L. L. Kee, C. Kirmaier, L. H. Lu, P. Thamyongkit, W. J. Youngblood, M. E. Calder, L. Ramos, B. C. Noll, D. F. Bocian, W. R. Scheidt, R. R. Birge, J. S. Lindsey and D. Holten, *J. Phys. Chem. B*, 2005, **109**, 20433–20443; (*b*) A. C. Benniston, A. Harriman, V. L. Whittle and M. Zelzer, *Eur. J. Org. Chem.*, 2010, 523–530; (*c*) D. P. Wang, R. Miyamoto, Y. Shiraishi and T. Hira, *Langmuir*, 2009, **25**, 13176–13182; (*d*) B. Yucel, B. Sanli, H. Akbulut, S. Ozbey and A. C. Benniston, *Org. Biomol. Chem.*, 2012, **10**, 1775–1784.
17 (*a*) M. A. H. Alamiry, A. C. Benniston, G. Copley, K. J. Elliott, A. Harriman and B. Stewart, *Chem. Mater.*, 2008, **20**, 4024–4032; (*b*) L. A. Brey, G. B. Schuster and H. G. Drickamer, *J. Chem. Phys.*, 1977, **67**, 2648–2650; (*c*) L. A. Brey, G. B. Schuster and H. G. Drickamer, *J. Am. Chem. Soc.*, 1979, **101**, 129–134.
18 G. Hummer, S. Garde, A E. Garcia, M. E. Paulaitis and L. R. Pratt, *J. Phys. Chem. B*, 1998, **102**, 10469–10482.
19 K. Vedam and P. Limsuwan, *J. Chem. Phys.*, 1978, **69**, 4762–4771.
20 M. A. H. Alamiry, J. P. Hagon, A. Harriman and R. Ziessel, *Chem. Sci.*, 2012, **3**, 1041–1048.
21 T. Annable, R. Buscall, R. Ettelaie and D. Whittlestone, *J. Rheol.*, 1993, **37**, 695–726.
22 B. J. Littler, M. A. Miller, C.-H. Hung, R. W. Wagner, D. F. O'Shea, P. D. Boyle and J. S. Lindsey, *J. Org. Chem.*, 1999, **64**, 1391–1396.
23 R. Ziessel, G. Ulrich and A. Harriman, *New J. Chem.*, 2007, **31**, 496–501.
24 T. N. Singh-Rachford, A. Haefele, R. Ziessel and F. N. Castellano, *J. Am. Chem. Soc.*, 2008, **130**, 16164–16165.
25 D. K. Zhang, V. Martin, I. Garcia-Moreno, A. Costela, M. E. Perez-Ojeda and Y. Xiao, *Phys. Chem. Chem. Phys.*, 2011, **13**, 13026–13033.
26 W. W. Qin, M. Baruah, M. Van der Auweraer and F. C. De Schryver, *J. Phys. Chem. A*, 2005, **109**, 7371–7384.

 This journal is © The Royal Society of Chemistry 2012

27 R. Englman and J. Jortner, *Mol. Phys.*, 1970, **18**, 145–181.
28 R. Bonnett, D. J. McGarvey, A. Harriman, E. J. Land, T. G. Truscott and U. J. Winfield, *Photochem. Photobiol.*, 1988, **48**, 271–276.
29 P. J. Flory, *Principles of Polymer Chemistry*, Cornell University Press, Ithaca, NY, 1953.
30 J. D. Ferry, *Viscoelastic Properties of Polymers*, 3rd Edition, John Wiley & Sons Inc., New York, 1980.
31 K. F. Dziubek and A. Katrusiak, *J. Phys. Chem. B*, 2008, **112**, 12001–12009.
32 B. Neumann and P. Pollmann, *Phys. Chem. Chem. Phys.*, 2001, **3**, 943–951.
33 J. Vacek and J. Michl, *Proc. Natl. Acad. Sci. U. S. A.*, 2001, **98**, 5481–5486.
34 G. Strang, *Introduction to Linear Algebra*, Wellesley-Cambridge Press, Boston, 1993.
35 I. Vinckier, P. Moldenaers and J. Mewis, *J. Rheol.*, 1996, **40**, 613–631.
36 J. Schroeder, V. H. Schiemann and J. Jonas, *J. Chem. Phys.*, 1978, **69**, 5479–5488.
37 (*a*) M. Fury and J. Jonas, *J. Chem. Phys.*, 1976, **65**, 2206–2210; (*b*) D. B. Bauer, J. I. Brauman and R. Pecora, *Annu. Rev. Phys. Chem.*, 1976, **27**, 443–484.
38 (*a*) D. Gaeckle and D. Patterson, *Macromolecules*, 1972, **5**, 136–140; (*b*) N. Vennemann, M. D. Lechner and R. C. Oberthur, *Polymer*, 1987, **28**, 1738–1744.
39 (*a*) J. Roots and B. Nystrom, *Macromolecules*, 1982, **15**, 553–559; (*b*) B. D. Freeman, D. S. Soane and M. M. Denn, *Macromolecules*, 1990, **23**, 245–250.
40 R. L. Cook, H. E. King Jr. and D. G. Peiffer, *Macromolecules*, 1992, **25**, 2928–2934.

Published on 22 August 2012 on http://pubs.rsc.org | doi:10.1039/C2RA20786A
Downloaded on 17 September 2012